Oxygen Contribution on Li-Ion Intercalation−Deintercalation in $LiCoO_2$ Investigated by O K-Edge and Co L-Edge X-ray Absorption Spectroscopy

Won-Sub Yoon and Kwang-Bum Kim

Division of Materials Science & Engineering, Yonsei University, Seoul 120-749, Korea

Min-Gyu Kim,* Min-Kyu Lee, Hyun-Joon Shin, Jay-Min Lee, and Jae-Sung Lee

Pohang Accelerator Laboratory and Department of Chemical Engineering, Pohang University of Science and Technology, Pohang 790-784, Korea

Chul-Hyun Yo

Department of Chemistry, Yonsei University, Seoul 120-749, Korea

Received: October 8, 2001

To investigate the electronic structure of the electrochemically Li-ion deintercalated $Li_{1-x}CoO_2$ system, soft X-ray absorption spectroscopy (XAS) for the oxygen K-edge and the Co $L_{II,III}$-edge has been carried out intensively with compositional x value variation, compared with Co K-edge X-ray absorption near edge structure (XANES) spectroscopy. To get reasonably good XAS spectra for the electrochemically Li-ion deintercalated $Li_{1-x}CoO_2$ system, we made a binder-free $LiCoO_2$ film electrode using the electrostatic spray deposition (ESD) technique. The oxygen K-edge XAS for $Li_{1-x}CoO_2$ shows more effective spectral change with respect to Li-ion content than the Co $L_{II,III}$-edge XAS. The dependence of the absorption peak feature on the Li content is described in terms of the ground state of the Co and O atoms, showing the systematic variation of the hole-state site distribution between Co and oxygen atoms. From the Co $L_{II,III}$-edge XAS, it is found that the broad peak shift to higher energy with the Li-ion deintercalation is due to rehybridization between Co and O atoms under the local structural distortion of CoO_6 octahedra, which is also confirmed by the formation of two additional absorption peaks below the threshold energy corresponding to the oxygen 2p hole state hybridized with the 3d orbital of Co ion in the distorted CoO_6 octahedral site. In the O K-edge XAS spectra for the deintercalated $Li_{1-x}CoO_2$ film, the shoulder absorption peak in the energy region higher than the threshold energy could be assigned to the higher oxidation state of the oxygen site on Li deintercalation. From the Co $L_{II,III}$-edge and O K-edge XAS results for the Li-ion deintercalated $Li_{1-x}CoO_2$ film, it is concluded that the charge compensation for the Li-ion deintercalation process could be achieved mainly in the oxygen site and Co metal atomic site simultaneously. O K-edge and Co $L_{II,III}$-edge XAS results for cycled $LiCoO_2$ film show that the capacity fading of the $LiCoO_2$ system is related to the decrease of Co−O bond covalency by the local structural distortion of CoO_6 octahedra remaining in the cycled $LiCoO_2$.

Introduction

A number of research on the electrochemical and physical properties of $LiCoO_2$ has been carried out for applications in view of its high energy density and stability. Further, $LiCoO_2$ has been used widely as an attractive material for rechargeable lithium battery cathodes owing to advantages such as the high working voltage and the reversible Li-ion intercalation.[1−7] As reported recently, a higher open-circuit voltage above ∼4.0 V is obtained both theoretically and experimentally by the substitution of nontransition metal ion like Al^{3+} for Co^{3+} ion.[8] In this case, it has been suggested that the electrochemical property of electron exchange is much associated with the participation of the oxygen 2p band, in addition to the charge compensation by the metal ion. It is very important to investigate the amount of oxygen atom contribution to the charge compensation during the Li-ion intercalation−deintercalation process. The conventional concept of this electrochemical reaction is that only the Co^{3+} ion in $LiCoO_2$ takes part in the charge compensation during the Li-ion intercalation−deintercalation process; i.e., it changes its oxidation state from Co^{3+} in $LiCoO_2$ to Co^{4+} in CoO_2 during charging. However, recent reports debate over whether there is a change in oxidation state of Co ions in $Li_{1-x}CoO_2$ as x increases. Nakai et al.[9,10] reported from their in-situ Co K-edge XANES spectra of $Li_{1-x}CoO_2$ that a positive shift in energy for the absorption spectrum reflects the progressive oxidation of the Co^{3+} ion to the Co^{4+} ion in $Li_{1-x}CoO_2$ with the deintercalation of Li and also accounts for the shortening of the Co−O distance. Balasubramanian et al.[11] also suggested with their in-situ Co K-edge XANES spectra of $Li_{1-x}CoO_2$ that a positive shift in the Co edge shows oxidation of Co during charging. On the other hand, Montoro et al.[12] suggested with their Co $L_{II,III}$-edge X-ray absorption results and the analysis using atomic multiplet and band structure calculations that the trivalent Co^{3+} low-spin state remains mostly unaffected by the Li deintercalation. Wolverton and Zunger[13] also reported that the Li-ion removal leads to the restoration of charge to Co site by a rehybridization of Co−O orbitals. They suggested using first-principles calculations that the charge

* To whom correspondence should be addressed. Tel: 82-54-279-1188. Fax: 82-54-279-1598. E-mail: mgkim@postech.ac.kr.

10.1021/jp013735e CCC: $22.00
Published on Web 02/16/2002

enclosed around the Co site is constant for all configurations, as the Li content is reduced from $x = 1$ to $x = 0$. In contrast, first-principles calculations by Aydinol et al.[14] showed that a large amount of Co^{3+} are oxidized to Co^{4+}. Hence, It is very important to investigate the quantity of oxygen atom contribution on the charge compensation during the Li-ion intercalation−deintercalation process.

Extensive research on the electronic structure of the Li-ion intercalated cathode material has been carried out. X-ray absorption spectroscopy (XAS) has been used for structure refinement on the transition metal ion of the cathode. The XAS study for the Li-ion intercalation−deintercalation has been mainly investigated from the viewpoint of the Co metal ion.[15,16] The absorption peak features of the Co K-edge XAS include useful structural information such as the oxidation state of the chemical species, their site symmetries, and covalent bond strength. In this case, the small preedge peak has been used to infer the electronic structure of the central atom since the transition is very sensitive to chemical environments despite the electric dipole-forbidden transition. From the peak position and intensity of the Co K-edge XANES spectra, it has been reported that the Li-ion deintercalation leads to the increase of the average oxidation state of the Co ion and the local structural distortion around the Co atom. However, the XANES spectra could not give any direct information for participation of oxygen in the charge compensation process. Only the contribution of the oxygen atom could be indirectly inferred from the peak intensity for electronic transition of the 1s electron to the 4p orbital with the shakedown process.

The quantitative study of electronic structures for various cobalt oxides has been carried out using the soft X-ray absorption spectroscopy technique.[17−23] Direct information of the unoccupied molecular level can be obtained from intensive absorption peaks of Co $L_{II,III}$-edge XAS representing the intense main 2p → 3d transition, unlike the weak preedge peak of 1s → 3d transition in Co K-edge XAS. The electric dipole-allowed 1s → 2p transition of oxygen K-edge XAS also provides a direct probe of the oxygen charge state and Co−O bonding interaction since the 2p orbitals of the oxygen ligand are involved in bonding configuration with Co metal ions under octahedral symmetry. The characteristic preedge features correspond to the electronic transition from the oxygen 1s core electron to the unoccupied molecular level by the hybridization of the Co 3d orbital with the oxygen 2p orbital. Therefore, the spectroscopic application of these soft X-ray absorptions to the $LiCoO_2$ system can be a useful tool that estimates the degree of oxygen contribution for the charge compensation in the Li-ion intercalation−deintercalation process.

Despite all the advantages of soft X-ray absorption for the investigation of the electronic structure of cobalt oxides, its application to the electrochemically Li-ion deintercalated $Li_{1-x}CoO_2$ system has been limited so far since the composite electrode consists of $LiCoO_2$ and some additives including organic binder and carbon, which could be a hindrance from getting reasonably good data. In the present study, we have made binder-free film electrode without any co-additives using the electrostatic spray deposition (ESD) technique. This makes possible more improved interpretation of O K-edge spectra for the electrochemically Li-ion deintercalated $Li_{1-x}CoO_2$ system. The electronic structures of the $Li_{1-x}CoO_2$ system have been investigated on the basis of Co $L_{II,III}$ and oxygen K-edge XAS studies, compared with Co K-edge XANES spectra, thereby giving a better understanding of electronic structure of the electrochemically Li-ion deintercalated $Li_{1-x}CoO_2$ system.

Experimental Section

Sample Preparation and Characterization. $LiCoO_2$ film has been prepared by the electrostatic spray deposition (ESD) technique. The working principles of the ESD technique have been described in the literature.[24,25] The stoichiometric amount of lithium nitrate and cobalt nitrate with the cationic ratio Li:Co = 1:1 was dissolved in absolute ethanol and mixed to obtain a homogeneous precursor solution. A high voltage between the nozzle and Pt foil substrate makes the precursor solution atomized at the orifice of the nozzle, generating a fine aerosol spray. The temperature of the substrate was kept at 300 °C during the deposition. The precursor solution was pumped at 2 mL/h for 1 h through a nozzle placed above the substrate. The $LiCoO_2$ precursor was deposited on the Pt substrate and annealed at 800 °C in air for 30 min. The homogeneous uniphase of the $LiCoO_2$ film has been identified with X-ray diffraction analysis. To minimize interference from the diffraction peaks of the Pt substrate, a grazing angle scan was made in which the angle of the incident radiation with respect to the plane of the substrate was fixed at 5°.

The Li-ion electrochemical deintercalation-reintercalation process has been performed as follows. A three-electrode electrochemical cell was employed for electrochemical measurements in which lithium foil was used for both reference and counter electrodes. The electrolyte was used with 1 M $LiClO_4$ in propylene carbonate (PC) solution. Cyclic voltammetry (CV) and galvanostatic charge/discharge experiments were carried out using a multichannel potentiostat/galvanostat. All the electrochemical experiments were carried out at room temperature in a glovebox filled with purified argon gas. The Li-ion deintercalation−intercalation processes in Li/1 M $LiClO_4$, PC/$LiCoO_2$ cell were carried out with a current density of 50 $\mu A/cm^2$ in a voltage region between 3.0 and 4.2 V. The successive Li-ion deintercalation−intercalation processes have been repeated 50 times (50 cycles). For XAS experiments, the cells were first charged to a desired value of deintercalated Li-ion content (x value) at a C/10 rate and then relaxed for 1 day. The electrochemical cells were disassembled in an argon-filled glovebox, and the $LiCoO_2$ electrodes were taken out of the cell. These electrodes were then washed with tetrahydrofuran and dried thoroughly in a vacuum.

XAS Measurement. The soft XAS measurements of the $Li_{1-x}CoO_2$ were performed on the U7 beamline in the storage ring of 2.5 GeV with the ring current 120−160 mA at Pohang Light Source (PLS), which is the third generation synchrotron radiation source.[26] The U7 beamline, which consists of 4.3 m long, 7 cm period undulator and the variable-included angle plane-grating monochromator, provides the highly brilliant and monochromatic linear-polarized soft X-ray for the high-resolution spectroscopy.[27] The O K-edge and Co $L_{II,III}$-edge XAS data were taken in a total electron yield mode, recording the sample current. The experimental spectra were normalized by reference signal from the Au mesh with 90% transmission. The energy calibrations for the O K-edge and Co $L_{II,III}$-edge were made using the L-edge data of pure V and Co metal foils, respectively. According to the measured photon absorption spectra specified as the inner shell electron excitation for the Ar, N_2, and Ne gases, the energy resolving power ($E/\Delta E$) in the entire measurement range was greater than 3000. The base pressure of the experiment chamber was in the 10^{-8} mbar range.

Co K-edge X-ray absorption spectra (XAS) have been taken on the BL3C1 beamline at PLS. The Si(111) double crystal monochromator has been employed to monochromatize the X-ray photon energy. A high order harmonic contamination was

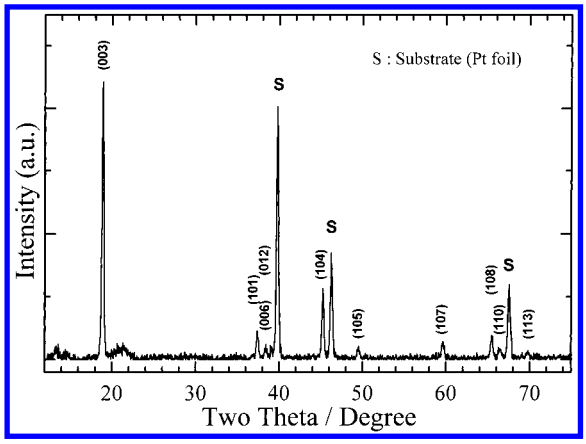

Figure 1. XRD pattern of $LiCoO_2$ film on Pt substrate annealed at 800 °C in air for 30 min.

eliminated by detuning the monochromator to reduce the incident X-ray intensity by ~30%. The incident X-ray intensity was monitored with a nitrogen gas-filled ionization chamber. The spectroscopic data have been collected in a total electron-yield mode. Energy calibration has been made using the Co metal standard foil. To collect the XANES spectra accurately for electronic transitions to specific bound states, the data have been taken with a step size of 0.2 eV in the XANES region. The data reduction of the experimental spectra was performed by the standard procedure reported previously.[15,16] The measured absorption spectra below the preedge region were fitted to a straight line, and then the background contribution above the postedge region was chosen using a third-order polynomial fitting. The polynomials of the extrapolated background were subtracted from the total absorption spectra and then the background-subtracted absorption spectra were normalized for a postedge energy region.

Results and Discussion

Characterization of $LiCoO_2$ Film. Figure 1 shows the XRD pattern for the $LiCoO_2$ film annealed at 800 °C in air for 30 min. All diffraction peaks can be indexed using the hexagonal axes option for the rhombohedral *R*3*m* space group. The XRD patterns for $LiCoO_2$ show the good separations of the (006)/(012) and the (108)/(110) couples of diffraction lines, which indicates that this material consists of a well-developed layered $LiCoO_2$.[28] It becomes clear that the oxygen octahedra of the central Co atom are edge-shared each other within the octahedral layer and the Li atoms are placed in the lattice channel between interlayer planes.

Figure 2 presents the cyclic voltammogram obtained from the $LiCoO_2$ film. The cyclic voltammogram was performed at a rate of 0.1 mV/s. Typical cyclic voltammograms of $LiCoO_2$ were observed, which were characterized by three sets of well-defined current peaks.[29] The $LiCoO_2$ film displays the main lithium intercalation and deintercalation peaks near 3.9 V, which is due to the coexistence of two pseudophases of an Li-dilute α-phase and an Li-concentrated β-phase. The separation between the anodic and cathodic peak was ca. 65 mV, indicating good electrochemical reversibility. Two high voltage peaks observed above 4 V may result from phase transition between ordered and disordered lithium ion arrangements in the CoO_2 framework.[30] To demonstrate the electrochemical rechargeability of $LiCoO_2$ film, test cells were cycled at a current density of 50 μA/cm^2 between 3.0 and 4.2 V at room temperature. Figure 3 shows the discharge capacity vs cycle number of the $LiCoO_2$ film. The initial specific discharge capacity was 139 mA h g^{-1},

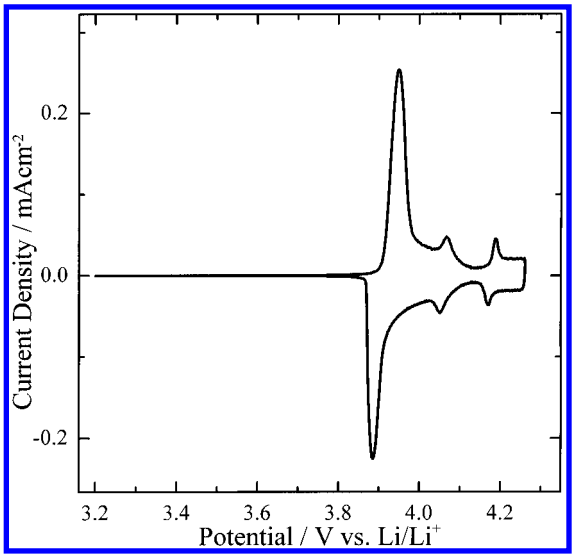

Figure 2. Cyclic voltammogram of $LiCoO_2$ film at a scan rate of 0.1 mV/s.

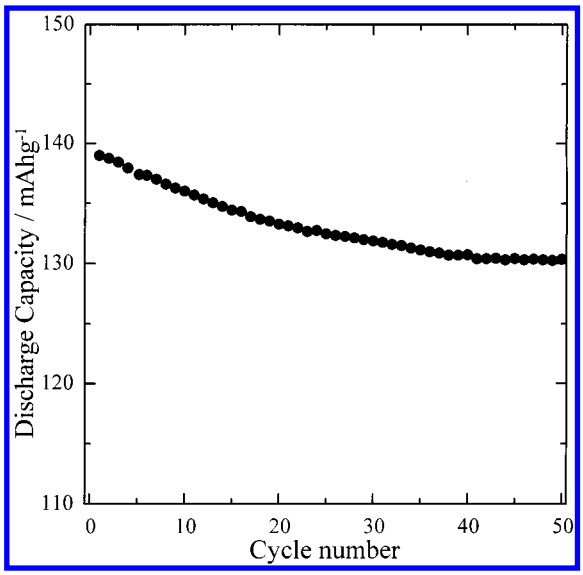

Figure 3. Discharge capacity vs cyclic number of $LiCoO_2$ film electrochemically cycled at the current density of 50 μA/cm^2 in the voltage range between 3.0 and 4.2 V.

which is close to the theoretical value of 137 mA h g^{-1} for exchange of 0.5 Li per CoO_2. As shown in Figure 3, the $LiCoO_2$ film deposited by the ESD method shows very stable electrochemical cycling characteristics.

Co $L_{II,III}$-Edge X-ray Absorption Spectroscopy. Figure 4 shows the Co $L_{II,III}$-edge X-ray absorption spectra of the $Li_{1-x}CoO_2$ system with respect to the *x* value. There are two main peaks of L_{III} and L_{II} edges that are due to electronic transitions of Co $2p_{3/2}$ and $2p_{1/2}$ core electrons, split by the spin−orbit interaction of the Co 2p core level, to an unoccupied 3d level highly hybridized with oxygen 2p orbital, respectively, as shown in Figure 5. For the Co^{3+} state in $LiCoO_2$, the corresponding electronic final states represent Co $2p^5c3d^7$-($t_{2g}^6e_g^1$), where the *c* represents the hole of the Co 2p core level. Since the absorption peaks are relatively intense by the electric dipole-allowed 2p → 3d transition and are very sensitive to the oxidation state, spin state, and bond covalency, the electronic structures of the Co ion in the $Li_{1-x}CoO_2$ system can be investigated qualitatively with peak features in the present soft X-ray absorption spectroscopic study.

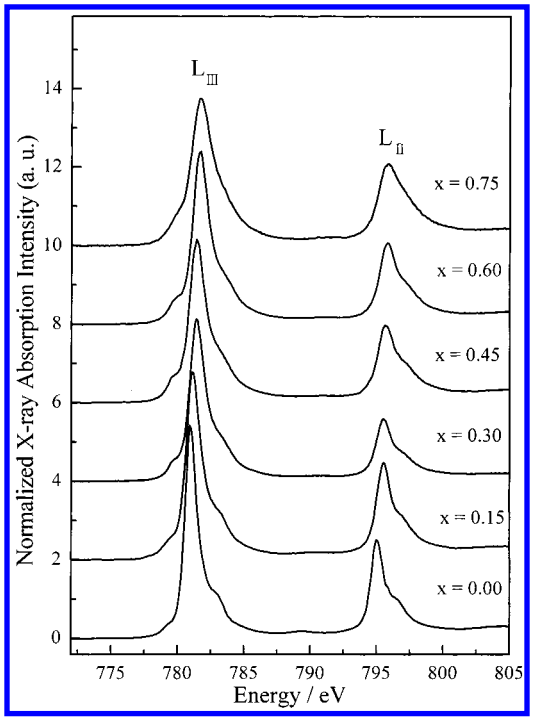

Figure 4. Normalized Co $L_{II,III}$-edge X-ray absorption spectra of $Li_{1-x}CoO_2$ system with respect to the *x* value.

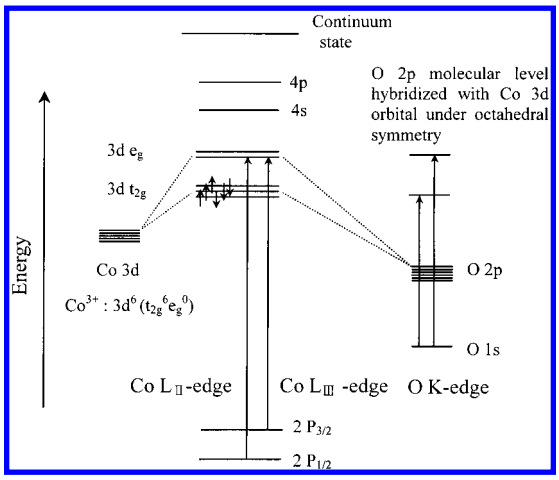

Figure 5. Schematic description of electronic transition in the preedge region of XAS spectra

The Co $L_{II,III}$-edge XAS of $LiCoO_2$ film is very similar to that of the bulk $LiCoO_2$ compound reported earlier.[22] The fact means that the $LiCoO_2$ film has been successfully prepared on the Pt substrate with the ESD method and there exists the Co^{3+} ion with only low spin configuration. The Co $L_{II,III}$-edge shows main peaks at ∼781 and ∼795 eV, and a weak shoulder peak at ∼782.8 and ∼796.6 eV, respectively, due to Co 2p−3d electrostatic interaction and crystal field effect of octahedral symmetry.

As shown in Figure 4, the Co $L_{II,III}$-edge XAS for the electrochemical deintercalation have been changed effectively with the *x* value. As the Li-ion deintercalation increases, the peaks are shifted and broaden toward the higher energy region, and its main peak intensity decreases. Figure 6 illustrates the relationship between the peak position and the deintercalated Li-ion content. At first, the linear relationship shows that the peak position is proportional to the *x* value of the $Li_{1-x}CoO_2$. The two possible structural effects give rise to the spectroscopic variation with respect to the *x* value. The charge compensation

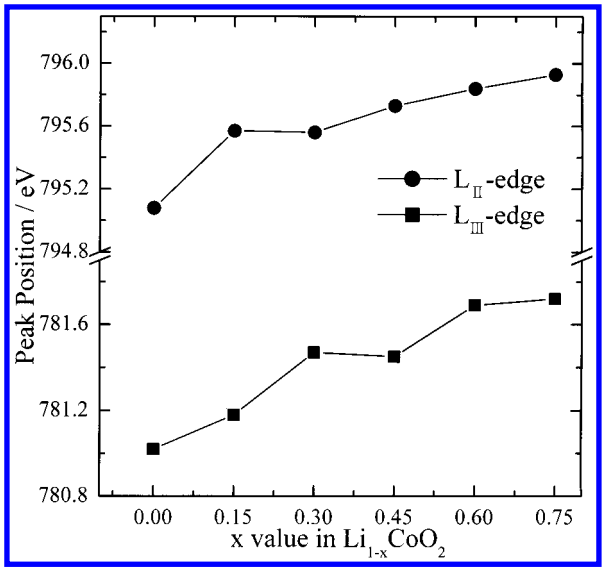

Figure 6. Relationship between the peak positions of Co $L_{II,III}$-edge X-ray absorption spectra and the deintercalated Li-ion content (x value).

is closely associated with two kinds of structural factors, i.e., rehybridization of Co−O molecular orbital and change in the effective nuclear charge of Co ion.

The first factor indicates that Co−O molecular orbital can be rehybridized in order to minimize the chemical perturbation by the Li-ion removal and store the charge to Co site, which is suggested by Zunger's group. The charge compensation can be accomplished by the local structural rearrangement of CoO_6 octahedra. Furthermore, according to the molecular orbital (MO) theory, the greater orbital overlap between Co 3d and O 2p orbitals results in an increase of both bond covalency and energy of the antibonding molecular level. The higher absorption energy is necessary for the 2p → 3d dipole transition in this case. Therefore, the peak feature for the higher Li-ion deintercalation shows the increase of Co−O bond covalency within the edge-shared CoO_6 octahedral layers. The second is conventional change in the effective nuclear charge of the Co ion. The positive charge deficiency by Li-ion removal can be compensated by the increased effective charge of Co ions. Considering the energy resolution (±0.1 eV), the contribution of the Co ion cannot be negligible on the charge compensation process for Li deintercalation. It is reasonable that the higher absorption energy is necessary for the Co ion under the higher oxidative environment in order to excite the 2p core electron, which is strongly bounded to the less screened nucleus. However, the distinct evolution of the Co^{4+} ion could not be observed with the broad Co $L_{II,III}$-edge peak feature, which means more oxidative Co ions are long-range disordered in the CoO_6 octahedral layer. As a result, the two structural factors participate in the charge compensation process effectively. The Li-ion deintercalation leads to the rehybridization of the Co−O molecular orbital due to the local structural distortion of CoO_6 octahedra as well as partial evolution in the increased effective nuclear charge of Co ion.

O K-Edge X-ray Absorption Spectroscopy. The O K-edge XAS of the electrochemically Li-ion deintercalated $Li_{1-x}CoO_2$ system have been shown in Figure 7. As the ligand K-edge XAS is very sensitive to the chemical environment around the ligand element, the electronic structure of the oxygen atom can be investigated intensively by the Li-ion content. According to previous ligand sulfur and chlorine K-edge spectroscopy for inorganic cluster complexes, the preedge peak position and intensity give important structural information about the chemical bonding between ligand and metal atoms. The preedge peak

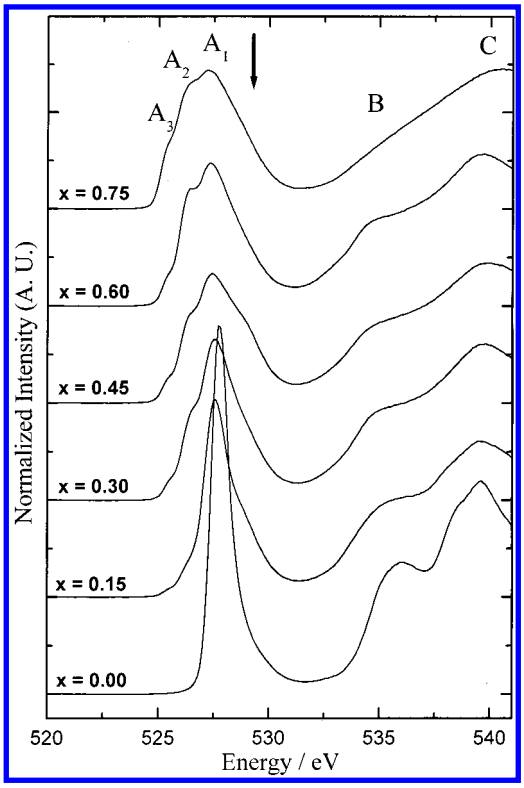

Figure 7. Normalized oxygen K-edge X-ray absorption spectra of $Li_{1-x}CoO_2$ system with respect to the *x* value.

position is related to the net formal charge variation of the ligand by the charge donation to the metal ion, the degree of d orbital splitting by the ligand field effect, and the overall d-mainfold energy by the effective nuclear charge of the metal ion. The peak intensity depends on the number of "d" hole states in the metal *n*d orbital hybridized with the ligand orbital and the bond covalency of the ligand−metal bond. In the present oxygen K-edge XAS study, therefore, the spectral change of the XAS for the Li-ion deintercalation can directly give useful structural information about the electronic structure of the oxygen ion and bonding character with the Co metal ion.

From the viewpoint of the localized nature of the oxygen 1s orbital, a symmetric and intense absorption peak (A_1 peak) at ~527.8 eV in the pristine $LiCoO_2$ represents the transition of the oxygen 1s electron to the hole state in the oxygen 2p level. The broad higher energy peaks (B and C peaks) above 536 eV can be assigned to the transitions to hybridized states of oxygen 2p and Co 4sp orbitals. In this case, the A_1 peak corresponds to the transition to an unoccupied molecular level, including Co 3d(e_g)−oxygen 2p character since the oxygen 2p orbital is highly hybridized with the 3d orbital of the Co^{3+} ion with low spin (t_{2g}^6, $^1A_{1g}$) electronic configuration under octahedral (O_h) symmetry. Although the oxygen 1s → Co 3d transition is forbidden by the electric-dipole approximation, the appearance of the absorption peak is due to the hybridization of Co 3d and oxygen 2p orbitals. The A_1 peak corresponds to a final state of O $1s^1c$ + Co $3d^7(t_{2g}6e_g^1)$ electronic configuration, where *c* is the oxygen 1s core hole.

As shown in Figure 7, the O K-edge XAS for Li-ion deintercalation have been changed effectively with the Li-ion content. The spectral changes of the O K-edge XAS are relatively more dramatic than those of the Co $L_{II,III}$-edge XAS with respect to the *x* value. The spectroscopic features give important information; e.g., the Li-ion deintercalation has a much larger influence on the electronic structure of the oxygen ion than on that of the Co ion. According to an earlier report, the electron exchange for charge compensation in the Li-ion electrochemical deintercalation−intercalation process occurs in the oxygen site as well as the Co atomic site, which is related to the higher operating voltage above ~4.0 V.[8,14] It has been suggested that the oxygen 2p band takes part in the electron exchange. In this study, the O K-edge XAS shows the direct responsibility of the oxygen 2p state on the bound state in the $Li_{1-x}CoO_2$ system.

The spectral changes of the O K-edge XAS are relatively more dramatic than those of the Co $L_{II,III}$-edge XAS with respect to the *x* value. The spectroscopic features show that the Li-ion deintercalation has a much larger influence on the electronic structure of the oxygen ion than on that of the Co ion. As the degree of electrochemical deintercalation increases (the *x* value increases), the A_1 peak intensity decreases gradually and an additional broad peak (marked by a vertical arrow) evolves as a shoulder peak in the higher region of ~1.2 eV. A chemical shift in the ligand 1s core energy is related to the effective charge on the ligand. The greater effective nuclear charge of the ligand in the more oxidative ligand site shifts the ligand preedge peak position to the higher energy region since the higher absorption energy is necessary for the more oxidized oxygen ion in order to excite the oxygen 1s core electron, which is strongly bound to the less screened nucleus. Therefore, the shoulder absorption peak in the energy region higher than the threshold energy can be assigned to the higher oxidation of the oxygen site on Li deintercalation, which indicates that the charge compensation for the electron exchange in the Li-ion deintercalation process could be achieved in the oxygen site. Our results are consistent with first-principles calculations of Ceder et al.[8,14]

On the other hand, the Li-ion deintercalation gives rise to the gradual formation of two additional well-resolved absorption peaks in the energy region lower than the threshold energy. The peak intensities increase systematically with Li-ion deintercalation. On the basis of the earlier reports of the ligand K-edge absorption,[31−35] the ligand preedge peak position shifts to the lower energy region due to both the local structural distortion and the increased effective nuclear charge of the metal ion. The peak intensity decreases with the bond covalency. The A_1 peak intensity decreases linearly with the *x* value, while the relative intensities of the A_2 and A_3 peaks increase. The variation of the peak intensity with the electrochemical deintercalation can give important structural information about the hole state distribution and the effective charge on the oxygen atom since the density of the empty bound state in the molecular energy level is related to the hybridization of Co 3d−O 2p orbitals.

The weak absorption peaks of $Li_{0.85}CoO_2$ compound, A_2 and A_3 peaks at ~525.8 and ~526.3 eV, are due to rehybridizations between the oxygen and the Co ion with the greater effective nuclear charge in the local distorted Co−O bond. The molecular rehybridization by the local structural distortion around the Co ion decreases the bond covalency. The gradual increase of A_2 and A_3 peak intensities with the Li-ion deintercalation shows the systematic increase of the molecular rehybridization and then decrease of bond covalency.

Figure 8 shows the normalized Co K-edge XANES of the $Li_{1-x}CoO_2$ system for comparison. The weak absorption peak A at ~7709.9 eV represents the transition of the 1s electron to an unoccupied 3d−e_g orbital of Co^{3+} ion with low-spin (t_{2g}^6, $^1A_{1g}$) electronic configuration. Although the 1s → 3d transition is an electric dipole-forbidden transition in an ideal octahedral symmetry, the appearance of the weak absorption peak is due to pure electric quadrupole coupling and the noncentrosymmetric environment of the slightly distorted CoO_6 octahedral site. Both

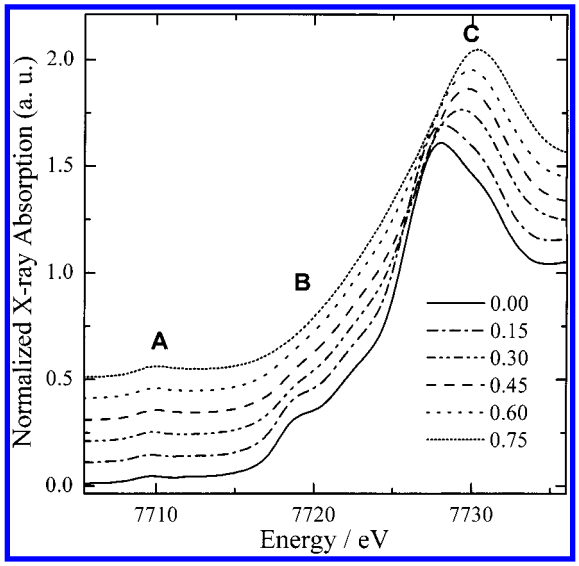

Figure 8. Relationship between the peak positions of oxygen K-edge X-ray absorption spectra and the deintercalated Li-ion content (x value).

B and C peaks appear by the electric dipole-allowed transition of a 1s core electron to an unoccupied 4p bound state with T_{1u} symmetry. The B and C peaks correspond to two final states of a $1s^1c3d^7L4p^1$ with the shakedown process by ligand to metal charge transfer (LMCT) and a $1s^1c3d^64p^1$ without the shakedown process, respectively, where *c* and *L* is a 1s core hole and a ligand hole. From the increase of the preedge peak intensity, the Li-ion deintercalation leads to local structural distortion around the Co atom, which is in good agreement with O K-edge results. The B peak disappears with the Li-ion deintercalation. This fact can be explained with the local structural distortion. Since the mismatched Co 3d−O 2p orbital overlap by the tilted arrangement of the CoO_6 octahedra leads to the decrease of the transfer integral, the LMCT process is difficult to occur in the higher deintercalation. Our results suggest that the Li-ion deintercalation leads to the local distortion of CoO_6 octahedral symmetry and the charge compensation for the electron exchange in the Li-ion deintercalation−intercalation process is achieved mainly at the oxygen site as well as the Co atomic site.

XAS Study for Capacity Fading of $LiCoO_2$. As discussed above, it becomes clear that the oxygen charge state participates in the charge compensation for the Li-ion deintercalation process. In the Li-ion reintercalation process, the oxygen contribution for the electron exchange can be discussed from the viewpoint of the electrochemical cycling property of the $LiCoO_2$ system. As shown in Figure 3, the discharge capacities after the L-ion deintercalation−reintercalation processes of 10 and 50 cycles are 136 and 130 mA h g^{-1} at the current density of 50 μA/cm^2 in the voltage range between 3.0 and 4.2 V, corresponding to the capacity fading of ∼2.2% and ∼6.5% with respect to that of the first cycled $LiCoO_2$, respectively. Although the cyclic property shows the good electrochemical performance, the small capacity fading must be due to the local structural variations around Co and oxygen ions. The relationship between the capacity fading and the structure can be investigated with the Co K-edge, L-edges, and the oxygen K-edge XAS features after an electrochemical process of 10 cycles, compared to those of the pristine $LiCoO_2$, as shown in Figure 9.

In the Co K-edge and Co $L_{II,III}$-edge XAS features of Figure 9a,b, on the whole, there is no substantial spectral change between the peak features for the electrochemical reactions after 10 cycles. For the Li-ion reintercalation, the Co K and L-edge

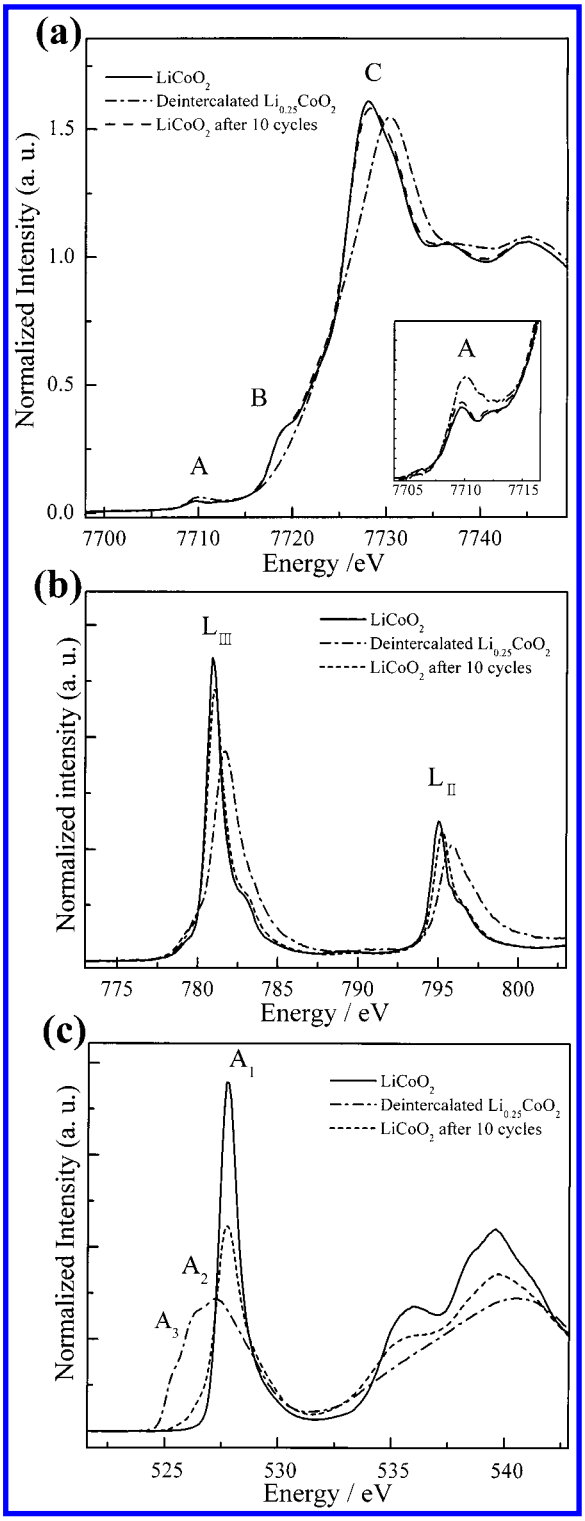

Figure 9. Comparison of X-ray absorption spectra in (a) Co K-edge, (b) Co $L_{II,III}$-edge, and (c) oxygen K-edge for the charge−discharge cycling property.

peaks of the $Li_{0.25}CoO_2$ shifted toward the higher energy region return reversibly to the peak features before the first Li-ion deintercalation. The fact implies that the electrochemical deintercalation−reintercalation process is totally reversible even after 10 cycles. The small differences between the peak intensities can only be observed at both the preedge peak and white line of Co K-edge XANES. The preedge peak intensity slightly increases and the white line intensity decreases with the electrochemical cycling number, which is due to the increase of the Co 3d−4p orbital mixing in proportion to the local

structural distortion around Co ions. The Co L-edges XAS of uncycled and cycled $LiCoO_2$ shows that the peak position shifts slightly toward the higher energy after 10 cycles. Therefore, it is found that the electron exchange for charge compensation through the Co ion is not perfectly reversible even in the reversible Li-ion intercalation−deintercalation process. The cyclic property of $LiCoO_2$ can be supported with the oxygen K-edge XAS. The whole peak features after 10 cycles are similar to that of uncycled $LiCoO_2$. However, the A_1 peak intensity corresponding to the transition to the oxygen 2p hole state decreases abruptly with the cycle numbers. According to the relationship between ligand K-edge peak intensity and bond covalency, the decrease of the peak intensity could be due to the decrease of Co−O bond covalency in the electrochemical cycled $LiCoO_2$. The peak feature can be explained with the local structure distortion of CoO_6 octahedra in the cycled $LiCoO_2$. Under the local distortion, the hole state in the oxygen 2p band by the LMCT process decreases in the cycled $LiCoO_2$ with respect to that of the uncycled compound. Therefore, the A_1 peak intensity of the oxygen K-edge decreases with the cycle number, which is related to the capacity fading of the $LiCoO_2$ system. In addition, the peak features after the electrochemical cycles show weak appearances of absorption peaks in the lower energy region below the threshold energy, indicating the existence of rehybridization between the Co 3d and O 2p orbitals. This shows the reversible redox reaction could not be perfectly carried out even in the ideal electrochemical deintercalation−intercalation processes.

Conclusion

The $LiCoO_2$ film electrode was successfully deposited on Pt foil by the electrostatic spray deposition technique. A cycling test showed that the $LiCoO_2$ film deposited by the ESD technique shows very stable cycling characteristics. The electronic structure for the electrochemically Li-ion deintercalated $Li_{1-x}CoO_2$ film has been investigated intensively with soft X-ray absorption spectroscopy (XAS) at the O K-edge and Co $L_{II,III}$-edge. From the observation of the Co $L_{II,III}$-edge, XAS results on Li-ion deintercalation, it is found that the contribution of the Co site on the charge compensation process for Li deintercalation cannot be negligible. This is confirmed by the evolution of two additional absorption peaks in the energy region lower than the threshold energy in the O K-edge spectra. In the O K-edge XAS spectra for the deintercalated $Li_{1-x}CoO_2$ film, the shoulder absorption peak in the higher energy region than the threshold energy could be assigned to the higher oxidation state of the oxygen site on Li deintercalation. It becomes clear that the charge compensation for the electron exchange in the Li-ion deintercalation process could be achieved in both the oxygen site and Co metal atomic site simultaneously. From O K-edge and Co $L_{II,III}$-edge XAS results for the cycled $LiCoO_2$ film, it is concluded that the capacity fading of the $LiCoO_2$ system could be related to the decrease of Co−O bond covalency by the local structural distortion of the Co site remaining in the cycled $LiCoO_2$.

Acknowledgment. The present study was supported by project No. 97-0501-0601-3 of the Korean Science and Engineering Foundation in 1999 and the Brain Korea 21 project. We are grateful to authorities of Pohang Light Source (PLS) for X-ray absorption spectroscopic measurements. This work was also supported in part by the Ministry of Information & Communication of Korea ("Support Project of University Information Technology Research Center" supervised by KIPA).

References and Notes

(1) Chiang, Y. M.; Jang, Y. I.; Wang, H. F.; Huang, B. Y.; Sadoway, D. R.; Ye, P. X. *J. Electrochem. Soc.* **1998**, *145*, 887.
(2) Ganguly, P.; Venkatraman, T. N.; Rajanohanan, P. R.; Ganapathy, S. *J. Phys. Chem. B* **1997**, *101*, 11099.
(3) Kumta, P. N.; Gallet, D.; Waghray, A.; Blomgren, G. E.; Setter, M. P. *J. Power Sources* **1998**, *72*, 91.
(4) Tukamoto, H.; West, A. R. *J. Electrochem. Soc.* **1997**, *144*, 3164.
(5) Dahn, J. R.; Van Sacken, U.; Juzkow, M. W.; Al-Janaby, H. *J. Electrochem. Soc.* **1991**, *138*, 2207.
(6) Ohzuku, T.; Ueda, A. *J. Electrochem. Soc.* **1994**, *141*, 2972.
(7) Numata, K.; Sakaki, C.; Yamanaka, S. *Chem. Lett.* **1997**, 725.
(8) Ceder, G.; Ching, Y. M.; Sadoway, D. R.; Aydinol, M. K.; Jang, Y. I.; Huang, B. *Nature* **1998**, *392* (16), 694.
(9) Nakai, I.; Takahashi, K.; Shiraishi, Y.; Nakagome, T. *J. Phys.IV* **1997,** *7*, C2−1243.
(10) Nakai, I.; Takahashi, K.; Shiraishi, Y.; Nakagome, T.; Nishikawa, F. *J. Solid State Chem.* **1998**, *140*, 145.
(11) Balasubramanian, M.; Sun, X.; Yang, X. Q.; McBreen, J. *J. Electrochem. Soc.* **2000**, *147* (6), 2903.
(12) Montoro, L. A.; Abbate, M.; Rosolen, J. M. *Electrochem. Solid State Lett.* **2000**, *3* (9), 410.
(13) Wolverton, C.; Zunger, A. *Phys. Rev. Lett.* **1998**, *81*, 606.
(14) Aydinol, M. K.; Kohan, A. F.; Ceder, G.; Cho, K.; Joannopoulos, J. *Phys. Rev. B* **1997**, *56* (3), 1354.
(15) Kim, M. G.; Yo, C. H. *J. Phys. Chem. B* **1999**, *103* (31), 6457.
(16) Yoon, W.-S.; Lee, K.-K.; Kim, K.-B. *J. Electrochem. Soc.* **2000**, *147* (6), 2023.
(17) van Elp, J.; Wieland, J. L.; Eskes, H.; Kuiper, P.; Sawatzky, G. A.; de Groot, F. M. F.; Turner, T. S. *Phys. Rev. B* **1991**, *44* (12), 6090.
(18) Abbate, M.; Fuggle, J. C.; Fujimori, A.; Tjeng, L. H.; Chen, C. T.; Potze, R.; Sawatzky, G. A.; Eisaki, H.; Uchida, S. *Phys. Rev. B* **1993**, *47* (24), 16124.
(19) Warda, S. A.; Massa, W., Reinen, D.; Hu, Z.; Kaindl, G.; de Groot, F. M. F. *J. Solid State Chem.* **1999**, *146*, 79.
(20) Montoro, L. A.; Abbate, M.; Rosolen, J. M. *J. Electrochem. Soc.* **2000**, *147* (5), 1651.
(21) Moodenbaugh, A. R.; Nielsen, B.; Sambasivan, S.; Fischer, D. A.; Friessnegg, T, Aggarwal, S.; Ramesh, R.; Pfeffer, R. *Phys. Rev. B* **2000**, *61* (8), 5666.
(22) Montoro, L. A.; Abbate, M.; Almeida, E. C.; Rosolen, J. M. *Chem. Phys. Lett.* **1999**, *309*, 14.
(23) Saitoh, T.; Mizokawa, T.; Fujimori, A.; Abbate, M.; Takeda, Y.; Takano, M. *Phys. Rev. B* **1997**, *55* (7), 4257.
(24) Chen, C.; Kelder, E. M.; van der Put, P. J. J. M.; Schoonman, J. *J. Mater. Chem.* **1996**, *6*, 765.
(25) Chen, C.; Kelder, E. M.; Kelder, M. J.; Jak, M. J. G.; Schoonman, J. *Solid State Ionics* **1996**, *86*−*88*, 1301.
(26) Lee, T. N.; Yoon, M. H.; Kim, Y. S.; Kim, H. G. *Austr. J. Phys.* **1995**, *48*, 321.
(27) Shin, H. J.; Chung, Y.; Kim, B. *J. Synchr. Radiation* **1998**, *5*, 648.
(28) Gummow, R. J.; Thackeray, M. M.; David, W. I. F.; Hull, S. *Mater. Res. Bull.* **1992**, *27*, 327.
(29) Uchida, I.; Saito, H. *J. Electrochem. Soc.* **1995**, *142*, L139.
(30) Reimiers, J. N.; Dahn, J. R. *J. Electrochem. Soc.* **1992**, *139*, 2091.
(31) Hedman, B.; Hodgson, K. O.; Solomon, E. I. *J. Am. Chem. Soc.* **1990**, *112*, 1643.
(32) Shadle, S. E.; Hedman, B.; Hodgson, K. O.; Solomon, E. I. *Inorg. Chem.* **1994**, *33*, 4235.
(33) Shadle, S. E.; Hedman, B.; Hodgson, K. O.; Solomon, E. I. *J. Am. Chem. Soc.* **1995**, *117*, 2259.
(34) Glaser, T.; Shadle, S. E.; Hedman, B.; Hodgson, K. O.; Solomon, E. I. *Acc. Chem. Res.* **2000**, *33* (12), 859.
(35) Glaser, T.; Shadle, S. E.; Hedman, B.; Hodgson, K. O.; Solomon, E. I. *J. Am. Chem. Soc.* **2001**, *123* (3), 442.